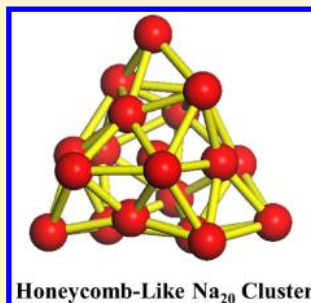


Evolution of the Structural and Electronic Properties of Medium-Sized Sodium Clusters: A Honeycomb-Like Na₂₀ ClusterWei Guo Sun,^{†,‡} Jing Jing Wang,^{¶,†} Cheng Lu,^{*,‡,§} Xin Xin Xia,[†] Xiao Yu Kuang,^{*,†} and Andreas Hermann^{*,||}[†]Institute of Atomic and Molecular Physics, Sichuan University, Chengdu 610065, China[‡]Department of Physics, Nanyang Normal University, Nanyang 473061, China[¶]Education College of Information Technology, Hubei Normal University, Huangshi 435002, China[§]Department of Physics and High Pressure Science and Engineering Center, University of Nevada, Las Vegas, Nevada 89154, United States^{||}Centre for Science at Extreme Conditions and SUPA, School of Physics and Astronomy, The University of Edinburgh, Edinburgh EH9 3JZ, United Kingdom**S** Supporting Information

ABSTRACT: Sodium is one of the best examples of a free-electron-like metal and of a certain technological interest. However, an unambiguous determination of the structural evolution of sodium clusters is challenging. Here, we performed an unbiased structure search among neutral and anionic sodium clusters in the medium size range of 10–25 atoms, using the Crystal structure AnaLYsis by Particle Swarm Optimization (CALYPSO) method. Geometries are determined by CALYPSO structure searches, followed by reoptimization of a large number of candidate structures. For most cluster sizes the simulated photoelectron spectra of the lowest-energy structures are in excellent agreement with the experimental data, indicating that the current ground-state structures are the true minima. The equilibrium geometries show that, for both neutral and anionic species, the structural evolution from bilayer structures to layered outshells with interior atoms occurs at $n = 16$. A novel unprecedented honeycomb-like structure of Na₂₀ cluster with C₃ symmetry is uncovered, which is more stable than the prior suggested structure based on pentagonal structural motifs.



1. INTRODUCTION

The geometric structure of atomic clusters' ground state is one of their most interesting properties and is a prerequisite to an accurate calculation of their electronic and other attributes.^{1–6} A large amount of work has been done, for instance, to determine the ground-state structures of small sodium clusters.^{7–12} Unfortunately, the lowest-energy structures of clusters are generally not amenable to direct experimental determination. Thus, it is customary to test the obtained structures indirectly, by comparing the experimental vertical detachment energy (VDE) and adiabatic detachment energy (ADE) with theoretical calculations.^{13,14} To thus confirm ground-state geometries, time-dependent density functional theory (TD-DFT) calculations can be performed to simulate the photoelectron spectrum (PES). The structure of the PES results from the superposition of the spectra of more or less different structures and can provide a detailed electronic fingerprint of those structures, as well as information on the isomerization dynamics.^{15–17}

Sodium in the extended state is one of the best representatives of a simple free-electron metal, in part because of the simple valence electron structure of sodium. Small sodium clusters have therefore received considerable attention from both the experimental and theoretical points of view.^{18–20}

In 1984,²¹ based on the discovery of “magic numbers” in the abundance spectra of Na_n with n up to ~100, Knight et al. established the spherical jellium model,^{22,23} which provides a simplified rule that the valence electrons of a cluster fill the spherical orbitals of a superatom according to the pattern of [1s²1p⁶1d¹⁰2s²1f¹⁴2p⁶1g¹⁸2d¹⁰...]. After this seminal discovery in sodium clusters, Bonaïć-Koutecký et al. explored computationally the relation between geometric structure and relative stability of small sodium clusters up to $n = 9$ and also demonstrated the complete analogy to the electronic properties of Li_n clusters.²⁴ The ground-state geometries of anionic sodium clusters ($n = 4–19$) were investigated by photoelectron spectroscopy and finite-temperature ab initio molecular dynamics calculations.¹⁴ The geometries of neutral and singly charged sodium clusters up to 20 atoms were also calculated systematically, and the influence of electronic correlation on the electronic structure and the dynamic properties of small sodium clusters was examined.²⁵ Quite recently, Nagare et al.²⁶ discussed the electronic structure and equilibrium geometries of sodium clusters in the size range from 2 to 20 atoms as a

Received: September 28, 2016

Published: January 20, 2017

function of confinement, relying on a real-space implementation of DFT.

Although tremendous progress has been made in the study of sodium clusters, especially regarding the geometric structures of small sodium clusters, the ground-state geometries and corresponding electronic properties of medium-sized clusters have so far resisted interpretation. For example, the fundamental properties of the lowest-energy Na_{20} cluster are still a subject of controversy.^{7,27} The main reasons may be summarized as follows: The procedure used to obtain structures of the small clusters is not practical for medium-size clusters. Besides, the predicted global minima are subtly sensitive toward chosen implementations of exchange-correlation effects in DFT or the molecular-orbital level of theory in wave-function-based calculations. Furthermore, the determination of true global minimum structures poses greater challenges due to the much increased complexity of the potential energy surface of the configurational space, together with an exponential increase of low-energy structures with the number of atoms in the cluster.²⁸

To systematically research the structural evolution and electronic properties of medium-sized sodium clusters, we performed extensive structure searches for neutral and anionic sodium clusters in the size range from 10 to 25, by combining the Crystal structure AnaLYsis by Particle Swarm Optimization (CALYPSO) searching method with DFT calculations. The first goal of our work is to gain a fundamental overview of the lowest-energy geometric structures of medium-sized sodium clusters. Second, we reexamine a number of neutral and anionic low-lying isomers of medium-sized sodium clusters that have been reported previously by experiments or density functional calculations. And third, we are motivated to explore the physical mechanism behind the electronic properties of medium-sized sodium clusters and provide relevant information for further theoretical and experimental research.

The organization of the present paper is as follows. In the next section, we present the brief description of the computational methodology, along with the technical details regarding the ground-state structure reoptimization. Results are presented and discussed in Section III. Finally, the main conclusions are summarized in Section IV.

2. COMPUTATIONAL DETAILS

The structure search is based on globally minimizing potential energy surfaces evaluated by DFT calculations through a generalized version of a particle swarm optimization (PSO) algorithm specific for cluster structure prediction, as implemented in the CALYPSO code.^{29–31} The prominent feature of this method is the capability of predicting the most stable structure depending only on the knowledge of the chemical composition. The validity of this method in structure prediction has been demonstrated by its application for the successful identification of the ground-state structures for various systems.^{32–35} Structure predictions of the neutral and anionic sodium clusters are performed for each cluster size $n = 10–25$. In each search, a sequence of 50 generations of structural candidates is followed to achieve convergence of the search. Each generation contains 30 structures, 60% of which are generated by PSO, while the others are generated randomly. Low-lying structures within 2 eV of the global minimum structure are reoptimized with subsequent frequency calculations. The low-lying candidate isomers for each size are further optimized using DFT within the hybrid B3LYP

functional,³⁶ as implemented in the Gaussian 09 suite of programs.³⁷ The all-electron basis set 6-311+G(d)³⁸ is selected for the determination of the lowest-energy structures of medium-sized sodium clusters. Different spin multiplicities are considered in the geometric optimization process, up to sextet (quintet) for odd (even) electron numbers. Meanwhile, harmonic vibrational frequencies are calculated to ensure that the obtained structures are local minima. The photoelectron spectra of the anionic sodium clusters, which provide information on not only the ground electronic state of the anionic but also the ground and excited electronic states of the neutral species, are simulated using the TD-DFT method³⁹ and compared with the experimental data.^{13,14} Each anionic cluster has a unique electronic structure, so the different isomers can be easily distinguished by their photoelectron spectra. Finally, chemical bonding analysis is performed by natural bond orbital (NBO) and adaptive natural density partitioning (AdNDP) methods.⁴⁰ To test the reliability of our calculations, we also performed geometric optimization for small neutral and charged sodium dimers (Na_2 , Na_2^- , Na_2^+) through different functionals with 6-311+G(d) basis sets. The calculated results are summarized in Table S1. It can be seen from Table S1 that the calculated bond length, vibrational frequency, dissociation energy, VDE, and ionization potential of the small sodium dimers based on B3LYP methods are in good agreement with the experimental values. In fact, the validity of the hybrid B3LYP functional for small and medium-sized sodium clusters has been confirmed and reported by Solov'yov et al.²⁵ and Chandrakumar et al.⁴¹ So, B3LYP/6-311+G(d) is the reasonable method for medium-sized sodium clusters, and it therefore has been selected in our following calculations.

3. RESULTS AND DISCUSSIONS

3.1. Geometric Structure. We used the scheme described in the previous section to obtain the global minimum structures of neutral and anionic sodium clusters in the size range of $10 \leq n \leq 25$. The lowest-energy structures for each size are displayed in Figure 1. The electronic states and point symmetries of these structures are given in the Table 1. Other low-lying isomers with their symmetries and relative energies are shown in Figures S1 and S2 in the Supporting Information.

It can be seen in Figure 1 that, with the exception of $n = 15$, 19, 24, the global minimum structures of neutral and anionic clusters are different. The structure of Na_{10} is found to be a bicapped antiprism with a bilayer structure, which is in full compliance with Solov'yov et al.²⁵ by using B3LYP/6-311+G(d), while Na_{10}^- preserves the bilayer trapezoidal shape. We notice that the energy of Na_{11} obtained here is only slightly lower than the metastable structure that is shown in Figure S1. $\text{Na}_{12–13}$ adopt oblate layer structures by fusing hexagonal polyhedron sodium units, while Na_{13}^- has a bilayer oblate structure with C_{2v} symmetry. For $n = 14–16$, all of the neutral structures adopt oblate shapes that can be viewed as sodium atoms capping the equatorial waist region of Na_{14} , while the anionic structures are deformations of the corresponding neutral structures, except for $n = 15$. The anions show a structural evolution pattern in agreement with previous findings by Moseler et al.¹⁴ For $n > 16$, the lowest-energy structures of neutral Na_n clusters are also in accordance with theoretical studies,⁷ with a few exceptions. A distinct structural evolution from bilayer structures to layered arrangements with interior atoms occurs at $n = 16$. The lowest-energy structures of the medium-sized anionic clusters are also in excellent agreement

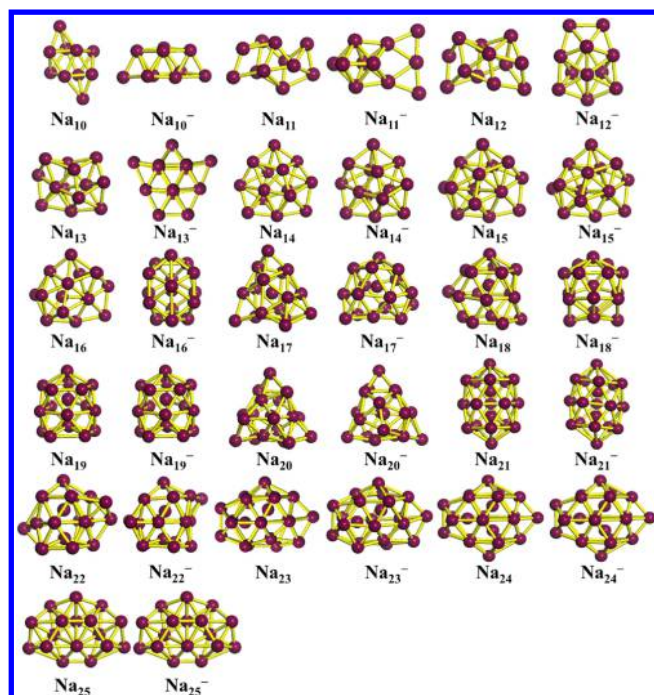


Figure 1. Lowest-energy structures of Na_n^Q ($n = 10\text{--}25$, $Q = 0, -1$) clusters.

with the previous works by Moseler¹⁴ and Aguado.⁷ On the basis of the jellium model,^{22,23} Na_{20} with a closed shell and 20 delocalized valence electrons (filling the superatom electronic shells as follows: $1s^2 1p^6 1d^{10} 2s^2$) exhibits an approximately spherical compact structure. The lowest-energy structure of Na_{20} here is, however, different from that of earlier studies.^{7,27,42,43} Previously, the C_s symmetry Na_{20} (Figure S1) was considered as the global minimum structure, with one atom capping the waist site of the double-icosahedron Na_{19} cluster. Here, however, we found that the most stable neutral honeycomb-like Na_{20} isomer has C_3 symmetry and is 0.016 eV lower in energy than the C_s structure, and a new

honeycomb-like structure is formed. To further confirm that the honeycomb-like Na_{20} structure is the true global minimum structure, many different functionals have also been examined, and the calculated results are listed in Table S2. However, on the basis of the calculations with both MP2 and CCSD, and 6-311+G(d) basis set, we found that the C_3 symmetry Na_{20} structure is always lower in energy than the previous C_s structure.^{7,27,42,43} The total energy difference is 0.065 eV (MP2) and 0.150 eV (CCSD), respectively. The optimized atomic coordinates along with the vibration frequency are given in the Tables S3 and S4. As for anionic Na_{20}^- , a structure with C_1 symmetry in pyramidal shape emerged as most stable. The C_{2v} structure of the Na_{21} isomer is based on a pentagonal prism with four atoms along the central internal axis, while Na_{21}^- forms a similar structure that distorts the neutral Na_{21} cluster's central axis. For $n = 22, 23$, the sodium cluster isomers contain two interior atoms, while for $n = 24, 25$ there are three interior atoms in double icosahedral structures. This structural evolution illustrates that interior atoms in the neutral clusters steadily descend into the icosahedral spherical structures with increased atom numbers. Anionic clusters with 22–25 atoms also prefer spherical and prolate structures derived from the compact double-icosahedron, differing only by slight distortions or minute changes in the positions of capping atoms from the corresponding neutral structures.

As stated above, the ground-state structures of the Na_n^Q ($n = 10\text{--}25$, $Q = 0, -1$) clusters evolve from bilayer structures to layered motifs with interior atoms for $n > 16$, based on icosahedral structures, and CALYPSO emerged as an elegant and effective approach to obtain the novel putative honeycomb-like Na_{20} cluster with C_3 symmetry.

3.2. Photoelectron Spectra of Na_n^- Clusters. Photoelectron spectroscopy is one of most significant experimental tools to get insight into, and to extract electronic binding energies from, a wide variety of atomic and molecular clusters as well as condensed-matter systems.^{14,44} To confirm the ground-state structures of the sodium clusters, the photoelectron spectra of the Na_n^- ($n = 10\text{--}25$) clusters are simulated using TD-DFT and compared to the available experimental

Table 1. Calculated Electronic States, Symmetries, Averaged Binding Energies (E_b), and HOMO–LUMO Energy Gaps (E_{gap}) for the Ground-State Na_n^Q ($n = 10\text{--}25$, $Q = 0, -1$) Clusters

Na_n					Na_n^-				
n	sta	sym	E_b	E_{gap}	n	sta	sym	E_b	E_{gap}
10	¹ A	C_2	0.568	1.31	10	² B	C_2	0.678	0.81
11	² A	C_1	0.566	0.88	11	¹ A ₁	C_{2v}	0.690	1.29
12	¹ A	C_2	0.585	1.36	12	² A'	C_s	0.680	0.82
13	² A	C_2	0.581	0.80	13	¹ A ₁	C_{2v}	0.693	1.37
14	¹ A	C_2	0.602	1.37	14	² A	C_2	0.684	0.77
15	² A	C_1	0.597	0.82	15	¹ A	C_1	0.689	0.97
16	¹ A	C_1	0.607	1.17	16	² A ₁	C_{2v}	0.688	0.79
17	² A	C_1	0.605	0.84	17	¹ A	C_2	0.696	1.10
18	¹ A	C_1	0.626	1.05	18	² A ₁	C_{2v}	0.706	0.75
19	² A'	C_s	0.630	0.79	19	¹ A'	C_s	0.707	1.11
20	¹ A	C_3	0.630	1.43	20	² A	C_1	0.699	0.74
21	² B ₂	C_{2v}	0.635	0.75	21	¹ A	C_2	0.697	0.83
22	¹ A	C_1	0.638	1.03	22	² A	C_1	0.696	0.69
23	² A	C_1	0.637	0.71	23	¹ A	C_1	0.699	0.83
24	¹ A ₁	C_{2v}	0.639	0.93	24	² B ₁	C_{2v}	0.693	0.67
25	² A ₂	C_1	0.638	0.73	25	¹ A ₁	C_{2v}	0.698	0.83

results. The simulated spectra together with the experimental PES data are displayed in Figure 2. The VDE is taken from the

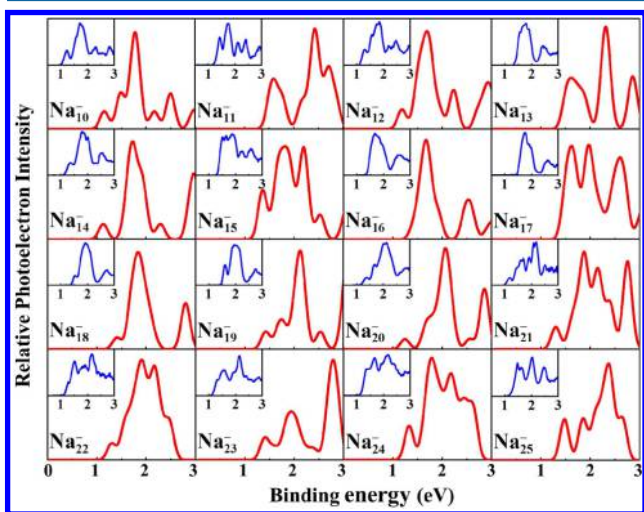


Figure 2. Simulated photoelectron spectra (red color) for Na_n^- ($n = 10-25$) clusters, along with the available experimental spectra (blue color) from Moseler¹⁴ ($n = 10-19$) and Huber¹³ ($n = 20-25$) for comparison.

first peak position of the spectra, and the ADE for the neutral clusters is obtained by the corresponding intersection between the baseline and the rising edge of the first peak.¹⁻³ The VDE and the ADE values are summarized in Table S5 in the Supporting Information, along with the experimental data^{13,14} for comparison. One can see satisfactory overall agreement between theoretical and experimental data, indicating the validity of our theoretical approach.

The simulated spectrum of Na_{10}^- shows three major peaks, and the first peak is located at 1.149 eV, which excellently reproduces the experimental features. In the simulated spectrum of Na_{11}^- , three peaks are also observed as in the experimental PES, although the first peak is moved to higher energy compared to experiment. The first weak peak on the simulated spectrum of Na_{12}^- emerges at 1.184 eV, followed by a broadened area and a distinct peak at 1.653 eV. The major peaks of experimental PES are successfully reproduced by theoretical calculation. In the case of Na_{13}^- , the simulated spectrum shows a broad peak at 1.509 eV, which presents the same characteristic as the experimental one. In the simulated spectrum of Na_{14}^- , it has a weak peak centered at 1.124 eV and an intense peak at 1.751 eV. Such three-peak behavior also occurred in experiment. The simulated spectrum of Na_{15}^- exhibits four major peaks, and the first peak appears at 1.361 eV, which is broadened into two peaks in experimental PES. A similar situation occurs for Na_{25}^- . For the PES of Na_{16}^- , both theoretical and experimental PES yield two peaks and have similar VDE value. In the simulated spectrum of Na_{17}^- , the first two peaks are separated by a valley, while these peaks merge together in experimental PES. For Na_{18}^- , the simulated spectrum excellently reproduces the experimental PES, and both of them present the same trend and yield three peaks. A similar situation occurs for Na_{19}^- , compared with the Na_{18}^- ; a weak shoulder emerges in the simulated spectrum of Na_{19}^- because of the appearance of a new 2S shell. In the simulated spectrum of Na_{20}^- , it also has four major peaks as observed in the experimental PES, while the second one is slightly narrow.

The simulated spectrum of Na_{21}^- shows a weak peak centered at 1.250 eV and an intense peak at 2.173 eV, which successfully reproduces the experimental characteristics. For Na_{22}^- , the simulated PES shows four major peaks, and the first is located around 1.298 eV. The simulated PES of Na_{23}^- exhibits three obvious peaks, and the first small peak appears at 1.378 eV, which is close to the experimental result. For Na_{24}^- , the simulated spectrum successfully reproduces the experimental spectrum; both of them show the same trend and yield three obvious peaks. The satisfactory agreement between simulated and experimental spectra within measurement error suggest that the lowest-energy structures of the sodium clusters are truly global minima. It should be pointed out that for some odd number of atom ($n = 11, 13, 15, \dots$) clusters, a more pronounced peak splitting is found in the simulated spectrum as compared to the experiment PES. This discrepancy between theory and experiment may be attributed to the following two aspects. In technical aspects, earlier works^{7,8,13,14} reported that sodium clusters at room temperature may be considered as liquidlike, and several degenerate isomers are explored, which state of the PES may cannot be well-produced. In theoretical aspects, the odd number of anionic clusters with closed electronic spin shell is more stable than the even clusters with the open spin shell, which is also the major factor for the discrepancy of sodium clusters with odd size.^{13,14,17}

3.3. Relative Stabilities of Na_n^Q ($n = 10-25$, $Q = 0, -1$).

The average binding energy (E_b) is representative of the intrinsic stability of sodium clusters, and it is calculated as

$$E_b(\text{Na}_n^Q) = [(n-1)E(\text{Na}) + E(\text{Na}^Q) - E(\text{Na}_n^Q)] / n \quad Q = 0, -1 \quad (1)$$

where E is the total energy corresponding to the respective neutral or anionic sodium clusters. E_b indicates the energy gain of adding a neutral or anionic Na atom to an existing cluster. As shown in Figure 3a, all of the neutral Na_n clusters have lower E_b values than their anionic states, suggesting it is always favorable to delocalize anionic charge in the clusters as opposed to a single atom. The curve of E_b shows opposite odd-even oscillating behaviors from $n = 10$ to 17 for neutral and anionic clusters: for the neutral Na_n clusters, the binding energy curves increase nonmonotonically with even maxima in the range of $n = 10-20$ and reach a global maximum at $n = 20$, followed by a flat energy trend for $n > 20$. As for anionic Na_n^- clusters, odd-size maxima are followed by a global maximum of 0.707 eV at $n = 19$. Thus, Na_{20} and Na_{19}^- are more stable than their adjacent clusters. This is in line with the explanation by closed-shell effects, which predict the stability of clusters with 20 valence electrons ($1s^2 1p^6 1d^{10} 2s^2$) by the spherical jellium model.

As is well-known, the second-order energy difference ($\Delta^2 E$) is another parameter that can reflect the relative stability of clusters. Figure 3b shows the size dependence of $\Delta^2 E$ for sodium clusters, where $\Delta^2 E$ is defined as

$$\Delta^2 E(\text{Na}_n^Q) = E(\text{Na}_{n-1}^Q) + E(\text{Na}_{n+1}^Q) - 2E(\text{Na}_n^Q) \quad Q = 0, -1 \quad (2)$$

The apparent peaks for the neutral sodium are formed at $n = 12, 14, 16, 18, 20, 22$, and 24, suggesting that even-sized clusters Na_n are of greater stability than neighboring odd-sized clusters. Moreover, the overall highest $\Delta^2 E$ value of Na_{20} again demonstrates its strong relative stability. The trend of the $\Delta^2 E$ curves is in accordance with the average binding energy. Except

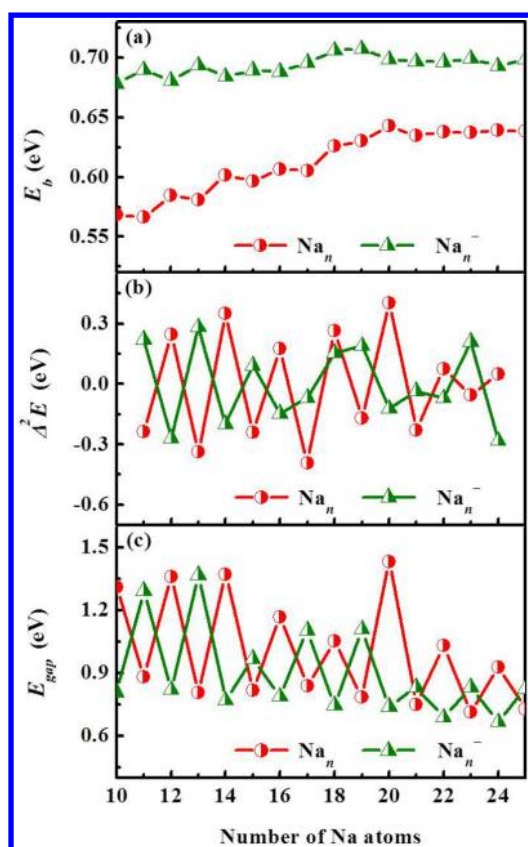


Figure 3. Size of dependence of (a) the average binding energies, (b) second-order energy differences, and (c) HOMO–LUMO energy gaps of Na_n^Q ($n = 10\text{--}25$, $Q = 0, -1$) clusters.

for Na_{18}^- , the anionic Na_n^- clusters show opposite odd–even oscillating trends compared to the neutral counterparts. Several distinct peaks of the $\Delta^2 E$ curve for anionic clusters indicate that $\text{Na}_{13,15,17,21,23}$ are more stable than the even-sized clusters. The same phenomenon has been reported by Aguado et al.⁷ and Huber et al.,¹³ based on the DFT level with exchange–correlation effects treated within the local density approximation.

The energy gap (E_{gap}) is another physical quantity that can reflect clusters' chemical stability, via the energy cost of an electronic excitation from the highest occupied molecular orbitals (HOMO) to the lowest unoccupied molecular orbitals (LUMO); higher values imply chemical inertness (or at least less reactivity). On this basis, the calculated E_{gap} values are listed in Table 1 and are also plotted in Figure 3c as a function of cluster size. We can clearly see that, for neutral clusters, the E_{gap} values of even-sized clusters are higher than for odd-sized clusters. This suggests that even clusters possess stronger chemical stability than their neighbors. As the neutral curve shows, the largest E_{gap} for neutral Na_n clusters occurs at $n = 20$, which is in accordance with the results from both E_b and $\Delta^2 E$. The number of valence electrons of Na_{20} is 20 ($1s^2 1p^6 1d^{10} 2s^2$), which exhibits the magic properties according to the jellium model. The variation of the E_{gap} values matches $\Delta^2 E$ as the cluster sizes increases. This suggests that cluster stability is driven by electronic, instead of structural, effects. Accordingly, for anionic clusters, the odd–even alteration behaviors of E_{gap} curve present the opposite trend compared to the corresponding neutral clusters: the values of E_{gap} show odd–even alterations with odd-sized maxima, where overall maxima

occur at $n = 11, 13, 17$, and 19 , which suggests that these clusters have stronger chemical stability than their adjacent clusters. On the basis of the above analysis, we can conclude that honeycomb-like Na_{20} is a unique magic cluster and should be highly stable and chemically inert. There is a less-distinct magic number effect for the anionic clusters, where Na_{11}^- and Na_{13}^- also exhibit significantly higher stability than others.

3.4. Chemical Bonding Analysis. To further elucidate the stability of the neutral magic Na_{20} cluster with C_3 symmetry, which features the highest electronic E_{gap} across all our neutral clusters structures, we analyze its bonding nature by displaying HOMO–LUMO molecular orbitals in Figure 4. Since sodium

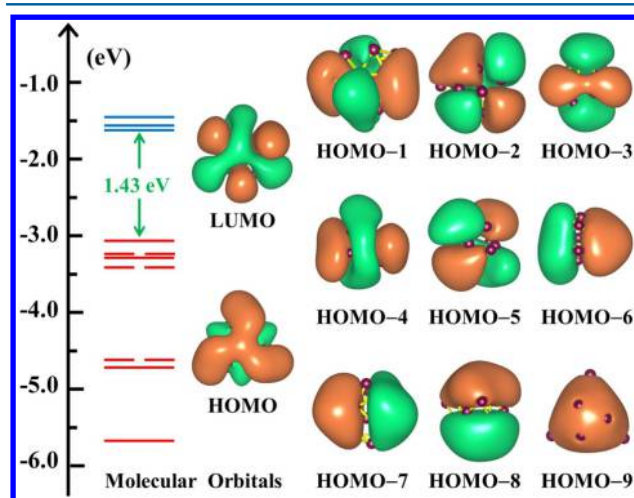


Figure 4. Molecular orbitals and energy levels of neutral Na_{20} cluster. The HOMO–LUMO energy gap is indicated (in green).

clusters can be viewed as typical model systems rationalized by the spherical jellium model, this can also be demonstrated by the occupied molecular orbitals. The nondegenerate HOMO is primarily a $2s$ -type atomic orbital, corresponding to the spherical shell structure within the peripheral and internal Na–Na bonds. Meanwhile, the LUMO resembles an f -type atomic orbital. The molecular orbitals of HOMO^q ($q = 1\text{--}5$) are d -type atomic orbitals: the HOMO-3 orbital exhibits the distinctive d_z^2 direction, while the other directions of d -atomic orbitals (such as d_{xy} , d_{yz} , $d_{x^2-y^2}$, and d_{zx}) feature in HOMO-1, HOMO-2, HOMO-4, and HOMO-5, respectively. The HOMO-6 to HOMO-8 orbitals are of p -type atomic orbital character (HOMO-8, for instance, can be assigned the p_z orbital). Lastly, the orbital of the HOMO-9 is a classical s -type atomic orbital within the spherical shell structure, and it is formed by σ NaNa bonds. We can deduce that the neutral Na_{20} cluster's electronic structure is best described as $1s^2 1p^6 1d^{10} 2s^2$, which is consistent with the HOMO, LUMO, and lower occupied molecular orbitals. The level degeneracies are broken by the nonspherical cluster geometry; however, some remain: the molecular orbitals of HOMO-1, HOMO-2, as well as HOMO-4, HOMO-5, HOMO-6, and HOMO-7 are degenerate. The large gap between the superatom $2s$ and $1f$ states is, to the best of our knowledge, the reason why the neutral Na_{20} exhibits the sizable energy gap of 1.43 eV between the HOMO–LUMO.

To gain alternate insight into the chemical bonding of neutral honeycomb-like $C_3\text{--Na}_{20}$, we performed chemical bonding analysis for Na_{20} by using the AdNDP method,^{45,46} which represents the bonding of a molecule in terms of localized and

delocalized n -center two-electron ($nc-2e$) bonds, with n potentially ranging from one to the total number of atoms in the systems. The detailed AdNDP analysis of the Na_{20} cluster is depicted in Figure 5, ordered by occupation number (ON).

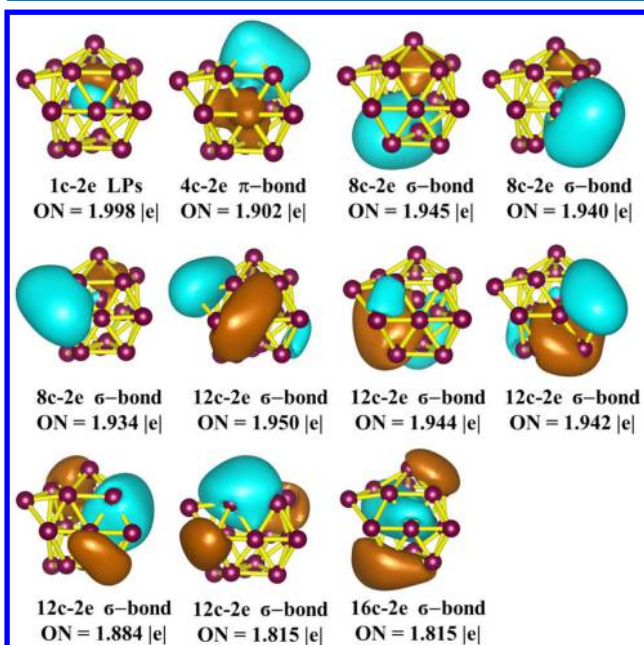


Figure 5. Chemical bonding analysis of the Na_{20} cluster using the AdNDP method. ON stands for occupation number.

The first bond depicts a lone pair on the internal Na with ON = 1.998 |e|, compared to 2.00 |e| in the ideal case, meaning that 0.002 |e| participates in π bonding with the surrounding sodium atoms. Moreover, the AdNDP reveals a 4c-2e π -bond describing stronger Na–Na bonds involving the three peripheral apex sodium atoms and the internal atom. The peripheral Na atoms contribute to the Na–Na bonds including delocalized bonding in the structure and form three 8c-2e σ -bonds with ON = 1.945 |e|, ON = 1.940 |e| and ON = 1.934 |e|, respectively. Additional delocalized bonding is provided in the shape of five 12c-2e σ -bonds with ON ranging from 1.815 |e| to 1.950 |e|. For each of these bonds, the internal sodium atom together with two peripheral sodium atoms contributes to the σ -bonds. The 16c-2e bond, finally, describes a σ -bond with the lowest occupation number ON = 1.815 |e|, where the internal atom forms a strong σ -bond and contributes to the high-energy gap in the Na_{20} clusters. Conceivably, most of the σ -bonds contribute to the substantial stabilization of the neutral $\text{C}_3\text{-Na}_{20}$ cluster.

3.5. Polarizability. The static electric dipole polarizability can determine the dynamical response of a bound system to external fields, and the analysis of atomic polarizabilities suggests a strong dependence on the structure of the clusters.^{27,47} For the curves shown in Figure 6, the polarizability per atom is defined in terms of the diagonal polarizability tensor components, and it is expressed as follows:

$$\bar{\alpha}/n = (\alpha_{xx} + \alpha_{yy} + \alpha_{zz})/3n \quad (3)$$

Here we present and analyze the results on the size dependence of the polarizabilities of Na_n^Q ($n = 10-25$, $Q = 0, -1$) clusters as determined from the respective lowest-energy structures. As illustrated in Figure 6, the overall polarizability

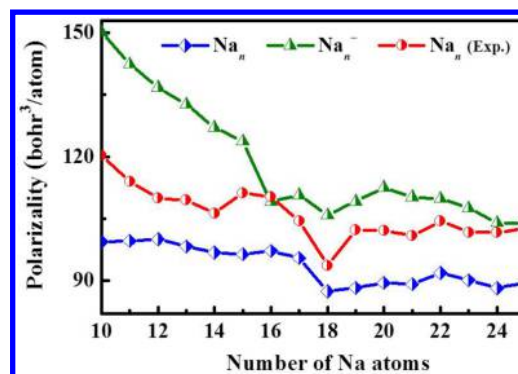


Figure 6. Polarizabilities per atom for Na_n^Q ($n = 10-25$, $Q = 0, -1$) clusters. The experimental data (in red) stem from Ma.²⁷

per atom is decreasing nonmonotonically with increasing cluster size n . Obviously, the values of anionic sodium clusters are higher than the neutral, and also demonstrate their sensitivity to the details of the cluster structure. The anisotropy of the anionic cluster structures is particularly sensitive to applied static electric fields. The neutral clusters' polarizability per atom from our calculations qualitatively reproduce the experimental data. But for all cluster sizes they consistently underestimate the measured values: by roughly 10 Bohr³ for most cluster sizes. This disparity are systematically discussed in by Ma et al.²⁷ and Kronik et al.⁴⁸ These calculations show that the quantitative discrepancy between theory and experiment is attributed to the effect of finite temperature and geometric evolution of the clusters structure. Somewhat generalizing, the polarizability also increases as the volume occupied by the electrons.⁴⁹ Therefore, the general downward trend of larger clusters indicates more tightly bound electrons, in contrast to the smaller clusters with only loosely bound electrons. The mean polarizability of sodium clusters in the regime of our research reduces toward a minimum corresponding to closed electronic shells, as well as a pronounced dip at $n = 18$, which has been interpreted intensively by Ma et al.²⁷ and Rayane et al.⁵⁰

4. CONCLUSIONS

In summary, a family of geometric structures and electronic properties of medium-sized sodium clusters Na_n^Q ($n = 10-25$, $Q = 0, -1$) has been acquired by CALYPSO searching method and subsequent DFT optimizations; the global minima of the neutral Na_{20} with C_3 symmetry has been proposed as a novel honeycomb-like isomer. Meanwhile, according to the considerable influence of the jellium model and electron shell structures, the structures evolve from bilayer structures to layered motifs with interior atoms relatively gradually for $n > 16$, with the latter based on icosahedral structures. The simulated photoelectron spectra show satisfying agreement with the experimental spectra for most sizes across the range of cluster sizes up to 25 atoms, which demonstrates that the structures we obtained are truly global minima. In particular, the Na_{20} cluster is found to be the most stable structure in the size range of $n = 10-25$ through an analysis of the relative stabilities. The lowest-energy structure of honeycomb-like Na_{20} , which also has a large HOMO–LUMO energy gap, is analyzed by natural bond orbital analysis and adaptive natural density partitioning. We constructed a computational polarizability evolution curve to compare with experiment and found that general features including the measured values were under-

estimated and that a significant polarizability minimum related to electronic shell closings at $n = 18$.

■ ASSOCIATED CONTENT

Supporting Information

The Supporting Information is available free of charge on the ACS Publications website at DOI: 10.1021/acs.inorgchem.6b02340.

The details of the low-lying isomers, the calculated VDE, ADE for the ground-state Na_n^Q ($n = 10\text{--}25$, $Q = -1$) together with the available experimental data and the Cartesian coordinates of Na_{20} cluster (PDF)

■ AUTHOR INFORMATION

Corresponding Authors

*E-mail: lucheng@calypso.cn. (L.C.)

*E-mail: scu_kuang@163.com. (K.X.Y.)

*E-mail: a.hermann@ed.ac.uk. (A.H.)

ORCID

Cheng Lu: 0000-0003-1746-7697

Notes

The authors declare no competing financial interest.

■ ACKNOWLEDGMENTS

This work was supported by the National Natural Science Foundation of China (Nos. 11574220, 11304167, 11274235, and 21671114), the 973 Program of China (No. 2014CB660804), the Special Program for Applied Research on Super Computation of the NSFC-Guangdong Joint Fund (the second phase), and the Program for Science & Technology Innovation Talents in Universities of Henan Province (No. 15HASTIT020). Part of the calculations were performed using the Cherry Creek Supercomputer of the UNLV's National Supercomputing Institute.

■ REFERENCES

- (1) Chen, J.; Zhang, Q. F.; Williard, P. G.; Wang, L. S. Synthesis and Structure Determination of a New Au_{20} Nanocluster Protected by Tripodal Tetrakisphosphine Ligands. *Inorg. Chem.* **2014**, *53*, 3932–3934.
- (2) Su, J.; Dau, P. D.; Qiu, Y. H.; Liu, H. T.; Xu, C. T.; Huang, D. L.; Wang, L. S.; Li, J. Probing the Electronic Structure and Chemical Bonding in Tricoordinate Uranyl Complexes UO_2X_3^- ($X = \text{F}, \text{Cl}, \text{Br}, \text{I}$): Competition Between Coulomb Repulsion and U–X Bonding. *Inorg. Chem.* **2013**, *52*, 6617–6626.
- (3) Alexandrova, A. N.; Zhai, H. J.; Wang, L. S.; Boldyrev, A. I. Molecular Wheel B_8^{2-} as a New Inorganic Ligand. Photoelectron Spectroscopy and ab initio Characterization of LiB_8^- . *Inorg. Chem.* **2004**, *43*, 3552–3554.
- (4) Shao, N.; Huang, W.; Gao, Y.; Wang, L. M.; Li, X.; Wang, L. S.; Zeng, X. C. Probing the Structural Evolution of Medium-Sized Gold Clusters: Au_n^- ($n = 27\text{--}35$). *J. Am. Chem. Soc.* **2010**, *132*, 6596–6605.
- (5) Pal, R.; Wang, L. M.; Pei, Y.; Wang, L. S.; Zeng, X. C. Unraveling the Mechanisms of O_2 Activation by Size-Selected Gold Clusters: Transition from Superoxo to Peroxo Chemisorption. *J. Am. Chem. Soc.* **2012**, *134*, 9438–9445.
- (6) Khetrapal, N. S.; Jian, T.; Pal, R.; Lopez, G. V.; Pande, S.; Wang, L. S.; Zeng, X. C. Probing the Structures of Gold–Aluminum Alloy Clusters Au_xAl_y^- : A Joint Experimental and Theoretical Study. *Nanoscale* **2016**, *8*, 9805–9814.
- (7) Aguado, A.; Kostko, O. First-Principles Determination of the Structure of Na_N and Na_N^- Clusters with up to 80 Atoms. *J. Chem. Phys.* **2011**, *134*, 164304.

- (8) Kostko, O.; Huber, B.; Moseler, M.; von Issendorff, B. Structure Determination of Medium-Sized Sodium Clusters. *Phys. Rev. Lett.* **2007**, *98*, 043401.

- (9) Aguado, A.; López, J. M. Small Sodium Clusters that Melt Gradually: Melting Mechanisms in Na_{30} . *Phys. Rev. B: Condens. Matter Mater. Phys.* **2006**, *74*, 115403.

- (10) Haberland, H.; Hippler, T.; Donges, J.; Kostko, O.; Schmidt, M.; von Issendorff, B. Melting of Sodium Clusters: Where Do the Magic Numbers Come from? *Phys. Rev. Lett.* **2005**, *94*, 035701.

- (11) Kohl, C.; Fischer, B.; Reinhard, P. G. Polarized Isomers of Na Clusters and Anomalous Magnetic Response. *Phys. Rev. B: Condens. Matter Mater. Phys.* **1997**, *56*, 11149–11154.

- (12) Itoh, M.; Kumar, V.; Adschiri, T.; Kawazoe, Y. Comprehensive Study of Sodium, Copper, and Silver Clusters over a Wide Range of Sizes $2 \leq N \leq 75$. *J. Chem. Phys.* **2009**, *131*, 174510.

- (13) Huber, B.; Moseler, M.; Kostko, O.; von Issendorff, B. Structural Evolution of the Sodium Cluster Anions Na_{20}^- – Na_{57}^- . *Phys. Rev. B: Condens. Matter Mater. Phys.* **2009**, *80*, 235425.

- (14) Moseler, M.; Huber, B.; Häkkinen, H.; Landman, U.; Wrigge, G.; Hoffmann, M. A.; Issendorff, B. V. Thermal Effects in the Photoelectron Spectra of Na_N^- Clusters ($N = 4\text{--}19$). *Phys. Rev. B: Condens. Matter Mater. Phys.* **2003**, *68*, 165413.

- (15) Wrigge, G.; Hoffmann, M. A.; Issendorff, B. Photoelectron Spectroscopy of Sodium Clusters: Direct Observation of the Electronic Shell Structure. *Phys. Rev. A: At, Mol, Opt. Phys.* **2002**, *65*, 063201.

- (16) Piazza, Z. A.; Hu, H. S.; Li, W. L.; Zhao, Y. F.; Li, J.; Wang, L. S. Planar Hexagonal B_{36} as a Potential Basis for Extended Single-Atom Layer Boron Sheets. *Nat. Commun.* **2014**, *5*, 3113.

- (17) Mundt, M.; Kümmel, S.; Huber, B.; Moseler, M. Photoelectron Spectra of Sodium Clusters: The Problem of Interpreting Kohn-Sham Eigenvalues. *Phys. Rev. B: Condens. Matter Mater. Phys.* **2006**, *73*, 205407.

- (18) Brack, M. The Physics of Simple Metal Clusters: Self-Consistent Jellium Model and Semiclassical Approaches. *Rev. Mod. Phys.* **1993**, *65*, 677–732.

- (19) De Heer, W. A. The Physics of Simple Metal Clusters: Experimental Aspects and Simple Models. *Rev. Mod. Phys.* **1993**, *65*, 611–676.

- (20) Knight, W. D.; Clemenger, K.; De Heer, W. A.; Saunders, W. A. Polarizability of Alkali Clusters. *Phys. Rev. B: Condens. Matter Mater. Phys.* **1985**, *31*, 2539–2540.

- (21) Knight, W. D.; Clemenger, K.; De Heer, W. A.; Saunders, W. A.; et al. Electronic Shell Structure and Abundances of Sodium Clusters. *Phys. Rev. Lett.* **1984**, *52*, 2141–2143.

- (22) Ekardt, W. Dynamical Polarizability of Small Metal Particles: Self-Consistent Spherical Jellium Background Model. *Phys. Rev. Lett.* **1984**, *52*, 1925–1928.

- (23) Ekardt, W. Work Function of Small Metal Particles: Self-Consistent Spherical Jellium-Background Model. *Phys. Rev. B: Condens. Matter Mater. Phys.* **1984**, *29*, 1558–1564.

- (24) Bonáič-Koutecký, V.; Fantucci, P.; Koutecký, J. Systematic Ab Initio Configuration-Interaction Study of Alkali-Metal Clusters. II. Relation Between Electronic Structure and Geometry of Small Sodium Clusters. *Phys. Rev. B: Condens. Matter Mater. Phys.* **1988**, *37*, 4369–4374.

- (25) Solov'yov, I. A.; Solov'yov, A. V.; Greiner, W. Structure and Properties of Small Sodium Clusters. *Phys. Rev. A: At, Mol, Opt. Phys.* **2002**, *65*, 053203.

- (26) Nagare, B. J.; Kanhere, D. G.; Chacko, S. Structural and Electronic Properties of Sodium Clusters Under Confinement. *Phys. Rev. B: Condens. Matter Mater. Phys.* **2015**, *91*, 054112.

- (27) Ma, L.; Jackson, K. A.; Wang, J. G.; Horoi, M.; Jelinek, J. Investigating the Metallic Behavior of Na Clusters Using Site-Specific Polarizabilities. *Phys. Rev. B: Condens. Matter Mater. Phys.* **2014**, *89*, 035429.

- (28) Yoo, S.; Zeng, X. C. Structures and Relative Stability of Medium-Sized Silicon Clusters. IV. Motif Based Low-Lying Clusters $\text{Si}_{21}\text{--}\text{Si}_{30}$. *J. Chem. Phys.* **2006**, *124*, 054304.

(29) Wang, Y. C.; Lv, J.; Zhu, L.; Ma, Y. M. Crystal Structure Prediction via Particle-Swarm Optimization. *Phys. Rev. B: Condens. Matter Mater. Phys.* **2010**, *82*, 094116.

(30) Wang, Y. C.; Lv, J.; Zhu, L.; Ma, Y. M. CALYPSO: A Method for Crystal Structure Prediction. *Comput. Phys. Commun.* **2012**, *183*, 2063–2070.

(31) Lv, J.; Wang, Y. C.; Zhu, L.; Ma, Y. M. Particle-Swarm Structure Prediction on Clusters. *J. Chem. Phys.* **2012**, *137*, 084104.

(32) Lu, S. H.; Wang, Y. C.; Liu, H. Y.; Miao, M. S.; Ma, Y. M. Self-Assembled Ultrathin Nanotubes on Diamond (100) Surface. *Nat. Commun.* **2014**, *5*, 3666.

(33) Zhu, L.; Liu, H. Y.; Pickard, C.; Zou, G. T.; Ma, Y. M. Reactions of Xenon with Iron and Nickel are Predicted in the Earth's Inner Core. *Nat. Chem.* **2014**, *6*, 645–649.

(34) Wang, H.; Tse, J. S.; Tanaka, K.; Iitaka, T.; Ma, Y. M. Superconductive Sodalite-Like Clathrate Calcium Hydride at High Pressures. *Proc. Natl. Acad. Sci. U. S. A.* **2012**, *109*, 6463–6466.

(35) Lv, J.; Wang, Y. C.; Zhu, L.; Ma, Y. M. Predicted Novel High-Pressure Phases of Lithium. *Phys. Rev. Lett.* **2011**, *106*, 015503.

(36) Lee, C.; Yang, W.; Parr, R. G. Development of the Colic-Salvetti Correlation-Energy Formula into a Functional of the Electron Density. *Phys. Rev. B: Condens. Matter Mater. Phys.* **1988**, *37*, 785–789.

(37) Frisch, M.; Trucks, G.; Schlegel, H.; Scuseria, G.; Robb, M.; Cheeseman, J.; Montgomery, J., Jr.; Vreven, T.; Kudin, K.; Burant, J. et al. *Gaussian 09*; Gaussian, Inc.: Wallingford, CT, 2009.

(38) McLean, A. D.; Chandler, G. S. Contracted Gaussian Basis Sets for Molecular Calculations. I. Second Row Atoms, $Z = 11-18$. *J. Chem. Phys.* **1980**, *72*, 5639–5648.

(39) Casida, M. E.; Jamorski, C.; Casida, K. C.; Salahub, D. R. Molecular Excitation Energies to High-Lying Bound States from Time-Dependent Density-Functional Response Theory: Characterization and Correction of the Time-Dependent Local Density Approximation Ionization Threshold. *J. Chem. Phys.* **1998**, *108*, 4439–4449.

(40) Zubarev, D.; Boldyrev, A. Developing Paradigms of Chemical Bonding: Adaptive Natural Density Partitioning. *Phys. Chem. Chem. Phys.* **2008**, *10*, 5207–5217.

(41) Chandrakumar, K. R. S.; Ghanty, T. K.; Ghosh, S. K. Relationship between Ionization Potential, Polarizability, and Softness: A Case Study of Lithium and Sodium Metal Clusters. *J. Phys. Chem. A* **2004**, *108*, 6661–6666.

(42) Röhrlisberger, U.; Andreoni, W. Structural and Electronic Properties of Sodium Microclusters ($n = 2-20$) at Low and High Temperatures: New Insights from Ab initio Molecular Dynamics Studies. *J. Chem. Phys.* **1991**, *94*, 8129–8151.

(43) Jackson, K.; Ma, L.; Yang, M.; Jellinek, J. Atomistic Dipole Moments and Polarizabilities of Na_N Clusters, $N = 2-20$. *J. Chem. Phys.* **2008**, *129*, 144309.

(44) Mundt, M.; Kümmel, S. Photoelectron Spectra of Anionic Sodium Clusters from Time-Dependent Density-Functional Theory in Real Time. *Phys. Rev. B: Condens. Matter Mater. Phys.* **2007**, *76*, 035413.

(45) Averkiev, B. B.; Zubarev, D. Y.; Wang, L. M.; Huang, W.; Wang, L. S.; Boldyrev, A. I. Carbon Avoids Hypercoordination in CB_6^- , CB_6^{2-} , and C_2B_5^- Planar Carbon-Boron Clusters. *J. Am. Chem. Soc.* **2008**, *130*, 9248–9250.

(46) Popov, I. A.; Jian, T.; Lopez, G. V.; Boldyrev, A. I.; Wang, L. S. Cobalt-Centred Boron Molecular Drums with the Highest Coordination Number in the CoB_{16}^- Cluster. *Nat. Commun.* **2015**, *6*, 8654.

(47) Bowlan, J.; Liang, A.; De Heer, W. A. How Metallic Are Small Sodium Clusters? *Phys. Rev. Lett.* **2011**, *106*, 043401.

(48) Kronik, L.; Vasiliev, I.; Jain, M.; Chelikowsky, J. R. Ab initio Structures and Polarizabilities of Sodium Clusters. *J. Chem. Phys.* **2001**, *115*, 4322–4332.

(49) Anslyn, E. V.; Dougherty, D. A. *Modern Physical Organic Chemistry*; University Science Books, 2006.

(50) Rayane, D.; Allouche, A. R.; Benichou, E.; Antoine, A.; Aubert Frecon, M.; Dugourd, P.; Broyer, M.; Ristori, C.; Chandezon, F.; Huber, B. A.; et al. Static Electric Dipole Polarizabilities of Alkali Clusters. *Eur. Phys. J. D* **2011**, *106*, 043401.